JET–P(97)14

2D Physical Optics Simulation of Fluctuation Reflectometry

G D Conway.

JET Joint Undertaking, Abingdon, Oxfordshire, OX14 3EA, UK.

Plasma Phyics Laboratory, University of Saskatchewan, Saskatoon, Canada

3rd Workshop on Microwave Reflectometry for Fusion Plasma Diagnostics
Madrid, May 5th – 7th 1997

July 1997

Abstract.

The two-dimensional physical optics model of fluctuation reflectometry is reviewed and selected case studies presented comparing simulation with experimental results. The case studies include coherent modes, broadband turbulence, radial correlation lengths, correlation profiles and asymmetries in the launch - receive geometry.

1. Introduction

The two-dimensional (2D) physical optics model has been used to study several problems in fusion plasma fluctuation reflectometry [1,2]. These studies include quantifying the wavelength response to transverse propagating coherent modes [3]; the effects of broadband turbulence [4,5]; and more recently, the measurement of radial correlation lengths [6]. The results in each case show that the modulation of the reflectometer phase signal depends not only on the plasma fluctuation amplitude, but also on 2D effects such as the illumination spot size and the fluctuation wavelength or spectral content. Measured correlation lengths are also subject to 2D effects, however the model offers a means of reconciling the discrepancies between lengths measured from amplitude fluctuations (homodyne systems) and phase fluctuations (heterodyne systems). These, together with new results from simulating transverse correlation reflectometry, and the crucial effects of antenna misalignment (i.e. asymmetries in launch and receive geometry) will be summarised in this paper. Confirmatory experimental evidence from the JET correlation reflectometer will also be presented in each case as a validation of the model. With the inclusion of asymmetry effects the physical optics model now offers a comprehensive and (almost) complete picture of the behaviour of fluctuation reflectometry.

2. The model

The principles and limitations of the model have been described in detail in the literature [3,6,7], but are briefly summarised as follows. The plasma cutoff layer is approximated to a thin distorted conducting surface. The phase and amplitude of the electric field of a microwave beam reflected or scattered from the surface are then calculated from the Helmholtz equation. General solutions are obtained using a far-field Greens function and a paraxial Gaussian incident microwave beam with a circular or elliptic cross-section. Plasma fluctuations are modelled as two-dimensional distortions in the surface. The two most important 2D effects, finite illuminated area and surface structure, are incorporated in the model together with basic reflectometer geometry parameters

(i.e. launch and receive angles). For simple cases the Helmholtz equation can be solved analytically, but for a direct comparison with experimental results a numerical solution is more appropriate. Here, the reflection layer is moved past the reflectometer beam to generate simulated reflectometer time signals which are then processed as if they were real experimental signals using standard data analysis techniques.

3. Coherent modes

For the simple case of a coherent plasma or MHD mode the surface distortion is modelled as a sine wave with a normalised wavelength Λ/λ and peak amplitude h/λ, where λ is the microwave wavelength. The simplest reflectometer geometry is assumed, that is normal incidence and backscatter $\theta_1 = \theta_2 = 0$ (i.e. a single launch/receive antenna, or monostatic configuration).

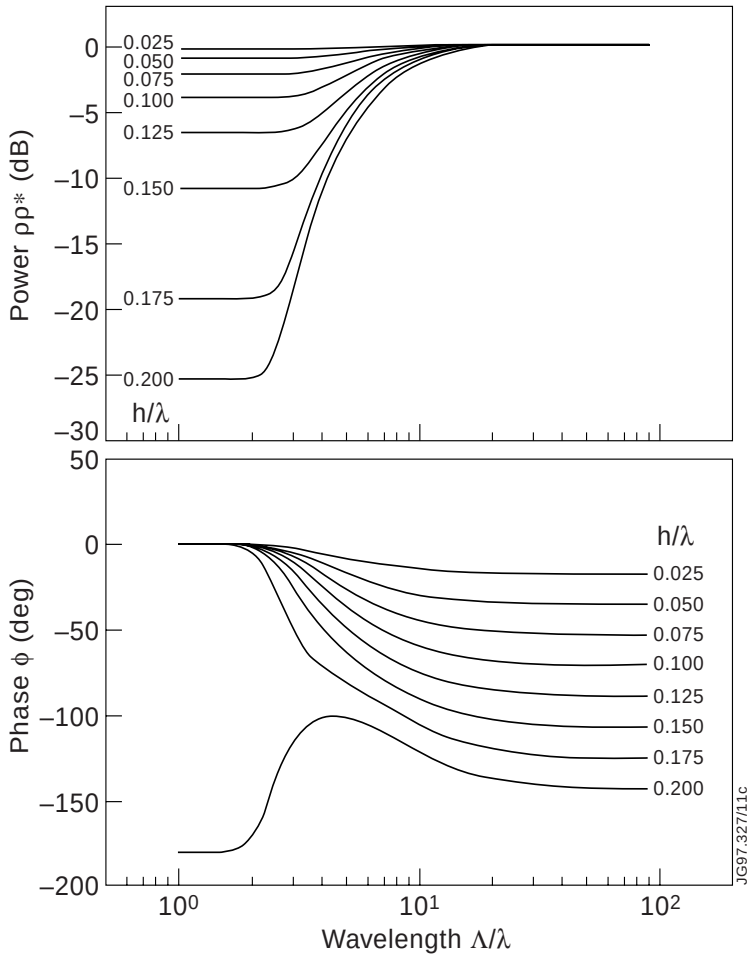

Figure 1: Simulation: Reflected power and peak phase shift vs normalised coherent mode wavelength Λ/λ as a function of mode amplitude h/λ with $w/\lambda = 2$. At large Λ/λ the results approach the 1D geometric optics limit.

(a) Simulation results.

Figure 1 shows the maximum reflected power and phase shift as a function of Λ/λ for increasing mode amplitude with a fixed Gaussian beam width $w/\lambda = 2$. There are three distinct wavelength regions which scale with the reflectometer beam radius [3]:

(a) Long fluctuation wavelengths: $\Lambda/\lambda >> 10\ w/\lambda$.

There is no attenuation, or modulation of the reflected power $\delta P = 0$. The phase shift replicates the shape of the mode, and the depth of phase modulation approaches the 1D geometric optics limit $\delta\phi = 4\ \pi\ h/\lambda$

(b) Transition wavelengths: $w/\lambda < \Lambda/\lambda < 10w/\lambda$.

Phase $\delta\phi$ is no longer linear with h/λ. The reflected power is attenuated and there is large δP modulation at twice the phase modulation frequency, $f_P = 2\ f_\phi$.

(c) Short wavelengths: $\Lambda/\lambda < w/\lambda$.

Both $\delta\phi$ and $\delta P \rightarrow 0$ with decreasing Λ/λ. The reflected power is strongly attenuated, saturating at a value determined by h/λ.

(b) Experimental results.

Figure 2 shows coherence spectra $\gamma^2(f)$ of phase and power signals from the JET correlation reflectometer (see accompanying paper for details [7]) with two beams separated by 40mm toroidally and the X-mode cutoff close to the plasma separatrix (R = 3.75m). The phase signal shows a coherent peak at 35kHz while the power signal shows a single peak at twice this frequency - as expected in the transition region. The time delayed cross correlation of the phase fluctuations shows a sinusoidal correlation with a temporal shift from zero of 18μs which gives a propagation velocity of $v = 0.04/18\mu s = 2.2 \pm 0.3$km/s. The reflectometer wavelength $\lambda = 4$mm and spot radius $w \approx 60$mm give a fluctuation wavelength of $\Lambda \approx 80$mm in the transition zone, and thus a propagation velocity of $v = \Lambda f = 2.8 \pm 0.6$km/s. The close agreement of the calculated and measured velocities, together with the frequency doubling in the power signal validates the model.

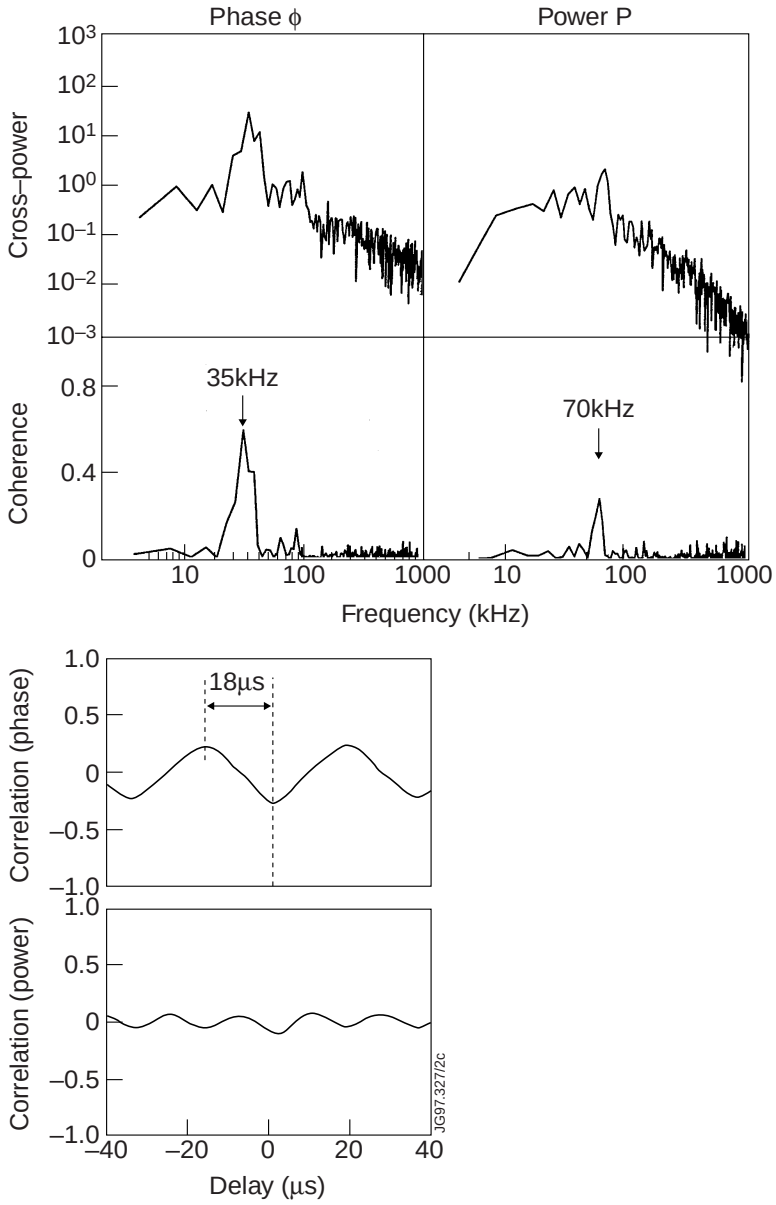

Figure 2: Experiment: Cross power and coherence spectra from JET edge showing coherent mode at 35kHz in phase signal and 70kHz mode in power signal. Phase cross correlation shows time delay of 18μs for 40mm toroidal separation. JET Pulse No. 38722, R~3.8m, t = 15.06–15.08s

4. Broadband turbulence

For broadband turbulence the surface distortions are simulated from Fourier components with a Gaussian wavenumber spectrum (normalised spectral width of k_w/k_o where $k_o = 2\pi/\lambda$) and an rms amplitude σ/λ. The reflectometer geometry is again a Gaussian beam normally incident on the reflection layer.

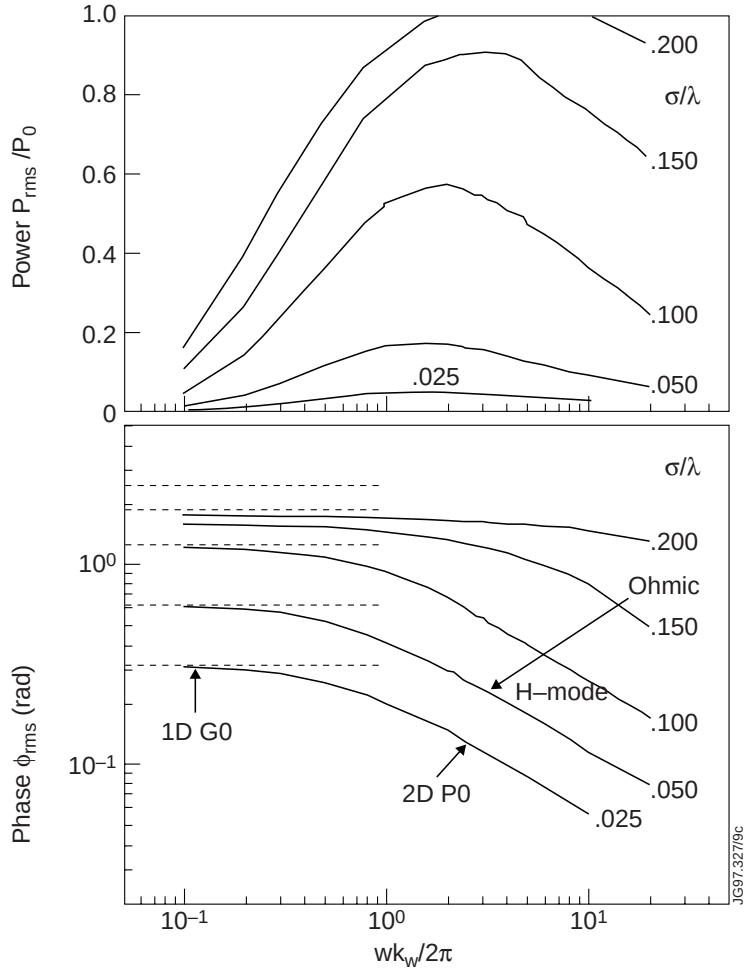

Figure 3: Simulation: rms phase and power from turbulent surface vs $k_w w/2\pi$ (beam width × spectral width) for increasing rms fluctuation amplitude σ/λ.

(a) Simulation results.

The random phase fluctuations in the reflected signal are symmetrically distributed (usually Gaussian) about the mean phase, but the power fluctuations are non-symmetrically distributed [5]. With increasing rms fluctuation amplitude σ/λ both the rms phase ϕ_{rms} and power P_{rms} levels initially increase and the mean reflected power level P_o decreases. For $\sigma/\lambda > 0.2$ the phase fluctuations become uniformly distributed between $\pm\pi$ and ϕ_{rms} goes to 0.6π. The spectral index also saturates at $n_\phi = -2$, i.e. a $1/f^2$ spectra; and P_{rms}/P_o approaches 1. Figure 3 shows the variation of ϕ_{rms} and P_{rms}/P_o as a function of the product of the beam radius and spectral width $(k_w/k_o) . (w/\lambda) = k_w w/2\pi$ for various values of σ/λ. For very long wavelength fluctuations, and very small spot sizes, $k_w w/2\pi << 1$ the power fluctuations go to zero $P_{rms}/P_o \rightarrow 0$ and the phase ϕ_{rms} approaches the 1D geometric optics limit $\phi_{rms} = 4\pi\sigma/\lambda$. However, for $k_w w/2\pi > 1$ and $\sigma/\lambda < 0.1$ the phase is given by:

$$\phi_{rms} = 4\pi \frac{\sigma}{\lambda} \frac{1}{\sqrt{2}} \left(\frac{k_w}{k_o} \frac{w}{\lambda} \right)^{-0.6} \qquad (1)$$

If *w* is known then measuring the rms phase and power levels will give the fluctuation amplitude and spectral width, and hence the transverse correlation length. σ is effectively the physical displacement of the reflection layer and is related to the rms density fluctuations $\tilde{n}$ (O-mode only) and magnetic field fluctuations B (X-mode reflectometer)

$$\sigma = L_n \frac{\tilde{n}}{n} \ (0-mode) \qquad \sigma = \frac{\tilde{n}/n + \tilde{B}/B(\omega_c\omega_c/\omega_p^2)}{L_n^{-1} + L_B^{-1}(\omega_c\omega_c/\omega_p^2)} \ (X-mode) \qquad (2)$$

Analysis of the signal spectra and distribution shape (skewness) of power fluctuations can also aid in determining plasma fluctuation properties.

(b) Experimental results.

Figure 4 shows a set of spectra and probability density functions (pdf) for reflectometer phase and power signals recorded during the ohmic and NBI heated H-mode phases from the JET edge (r/a ~0.9) region. As the edge turbulence decreases (predominantly low frequencies) in the H-mode, the ϕ_{rms} drops and the power pdf becomes more symmetric - exactly as predicted by the model [5]. All JET data follows the model, when the phase fluctuations increase the mean power decreases and visa versa. Using the curves in figure 3 the edge σ/λ is seen to drop from 18% to around 6%.

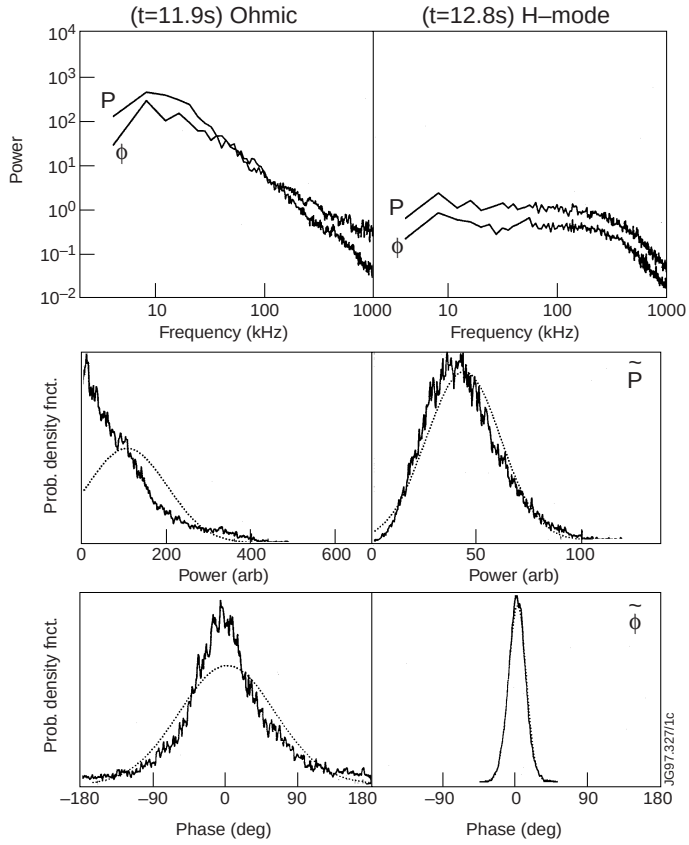

Figure 4: Experiment: Spectra and probability density functions (pdf) for JET edge fluctuations during ohmic (left) and NBI H-modes (right). JET Pulse No. 38369, R~3.8m

5. Radial correlation lengths

By extending the surface model to include a radial wavenumber component the model can be used to compare the radial correlation lengths of turbulence given by the phase signal $L_{r\phi}$ and the power signal L_{rP}. $L_{r\phi}$ is the value measured by heterodyne detection systems while L_{rP} is indicative of homodyne system results [6].

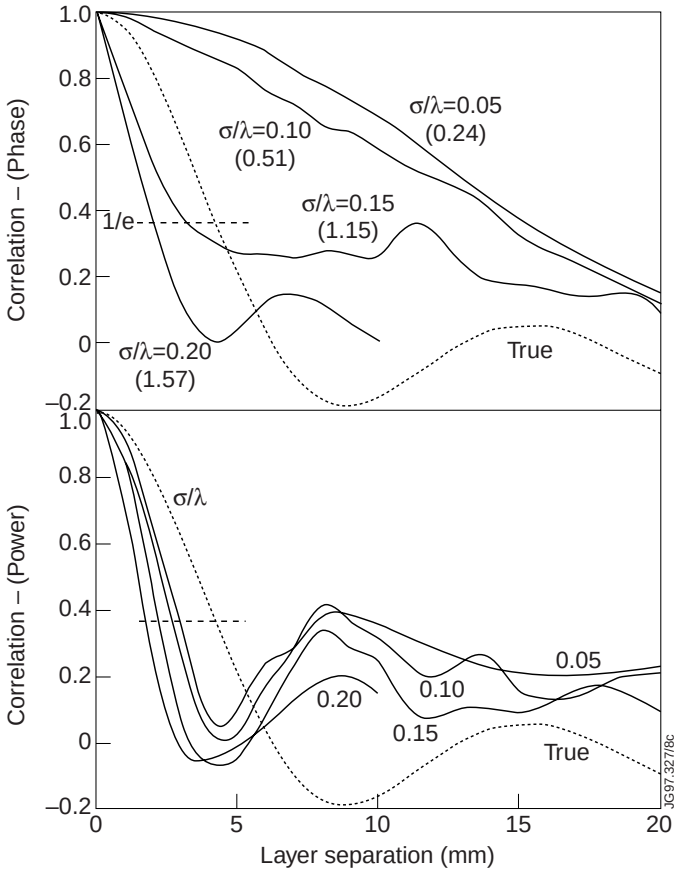

Figure 5: Simulation: Comparison of cross correlation coefficients vs radial separation from phase fluctuations (Top) and power fluctuations (Bottom) for increasing turbulence rms amplitude σ/λ. The dotted line is the true correlation function. $w/\lambda = 4$, $k_p/k_o = 0.35$, $k_r/k_o = 1.4$. Numbers in brackets are ϕ_{rms}

(a) Simulation results.

$L_{r\phi}$ and L_{rP} are generally different and not equal to the true correlation length $L_{r\ true}$. Figure 5 shows the effect of increasing the fluctuation amplitude σ/λ on the radial cross-correlation functions from the phase fluctuations (Top) and the power fluctuations (Bottom).

(a) For phase signals, $L_{r\phi}$ depends on σ/λ, w/λ and k_w/k_o. However these parameters also change ϕ_{rms} resulting in an 'empirical' scaling relationship:

$$L_{rtrue} = L_{r\phi}\left(\frac{\phi_{rms}}{\phi_c}\right)^b \qquad \text{where } \phi_c \approx \pi/3 \text{ and } b \approx \sqrt{3}$$

(b) For power and homodyne signals, L_{rP} only depends only slightly on σ/λ. The scale factor S ranges from $\sqrt{2}$ for small σ/λ (5%) to 2 for large σ/λ (>20%).

$$L_{rtrue} = L_{rP} \text{ x } S$$

(b) Experimental results.

Figure 6 shows contour plots of coherence spectra $\gamma^2(f)$ and time histories of $\bar{\gamma}^2$ for phase and power signals from the 92GHz JET radial correlation reflectometer with a constant layer separation of $\Delta r \approx 2.5$mm. In this ELMy H-mode the background coherence is generally low, except for two bursts of coherent activity around 19.02 and 19.06 seconds. Assuming Gaussian turbulence the radial correlation length is given by: $L_r = \Delta r\,(1 - \bar{\gamma})^{-1/2}$, which gives the values shown in the figure. Applying the scaling relationships to the $L_{r\phi}$ and L_{rP} values with a measured $\phi_{rms} \approx 90^o$ give the corrected true correlation lengths of 10mm and 7mm for the two bursts.

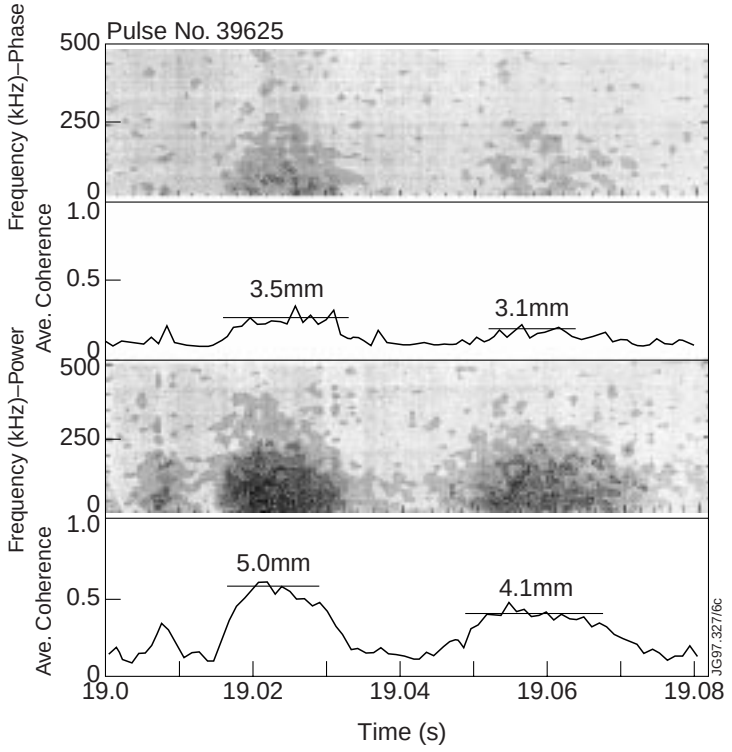

Figure 6: Experiment: Time evolution of $\gamma^2(f)$ coherence spectra for phase and power fluctuations from JET edge during two bursts of coherent mode activity (ELMy H-mode). R = 3.7m, Δf = 0.5GHz $\rightarrow \Delta r \approx$2.5mm.

6. Correlation profiles

The scaling laws derived above for the phase and power radial correlation lengths are also found to apply to correlation lengths for transverse separations, i.e. poloidal and toroidal correlation reflectometry with two separate microwave beams, and, to the time-delayed auto correlation functions, i.e. the phase and power auto-correlation times are different. All these effects are confirmed by experimental results. Another common feature in ***all*** correlation functions is the change in correlation profile of the phase fluctuations. For low fluctuation amplitudes $\sigma/\lambda \leq 0.1$ the phase signals have a Gaussian shape $C(x) = \exp(- x^2/L^2)$ for the initial decay, figure 7, but this changes to Lorentzian $C(x) = \exp(-x|/L|)$ for $\sigma/\lambda > 0.12$ or for $k_w w/2\pi < 0.05$. The auto-correlation profile shape can therefor also be used as an indication of the fluctuation level.

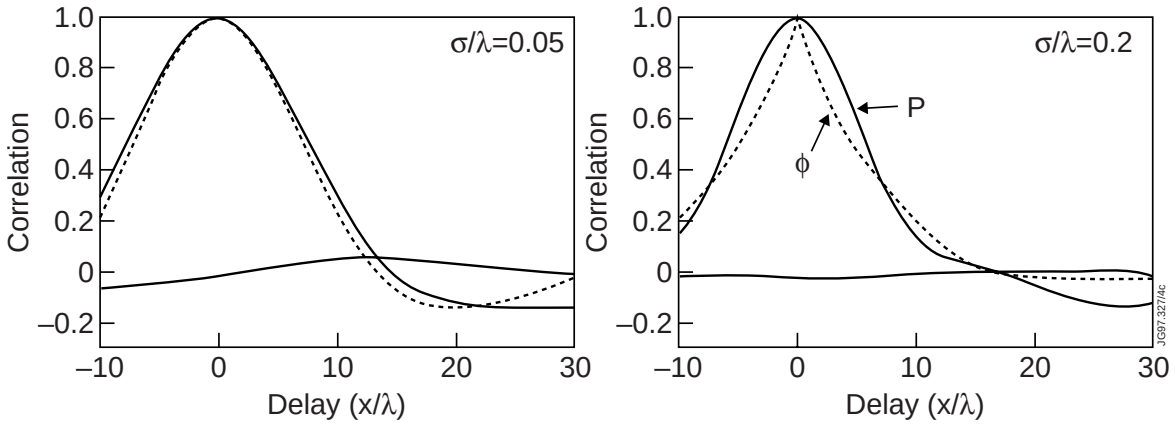

Figure 7: Simulation: Auto correlation functions of phase (dotted) and power (solid) fluctuations for $\sigma/\lambda = 0.05$ (left) and $\sigma/\lambda = 0.20$ (right). Normal incidence.

7. Asymmetries

Asymmetry can take several forms, such as non-symmetric plasma perturbations (i.e. sawtooth structures, rotating islands, etc.) or from antenna mis-alignments. Experimentally it is very difficult to maintain perfect symmetry between the plasma reflection layer and the antenna beams - that is a normally incident, and hence normally reflected beam in a single antenna (monostatic) system, or symmetric incident and reflected angles (relative to the layer) in a dual antenna (bistatic) system. For instance tilting of the reflection layer by just a few degrees from an initially symmetric system introduces a range of new effects, many of which are interrelated.

(a) Simulation results.

Extensive simulations with various asymmetries have been performed [8]. The following is just a brief summary of the more prominent features which appear with tilting the plasma reflection layer by an angle θ:

(a) For coherent modes, phase run-away occurs when the fluctuation amplitude exceeds a critical value. This value varies with the tilt or mis-alignment angle θ and the fluctuation wavelength. Figure 8 shows phase run-away occurring for $h/\lambda > 0.12$ with a θ of only 2.5^{o}.

(b) The long wavelength Λ sensitivity is lost with increasing θ.

(c) The phase shift ϕ no longer follows the surface but becomes distorted. This is evident in figure 8 as the perturbation moves through one period.

(d) At large Λ/λ the reflected power is strongly modulated at the perturbation frequency.

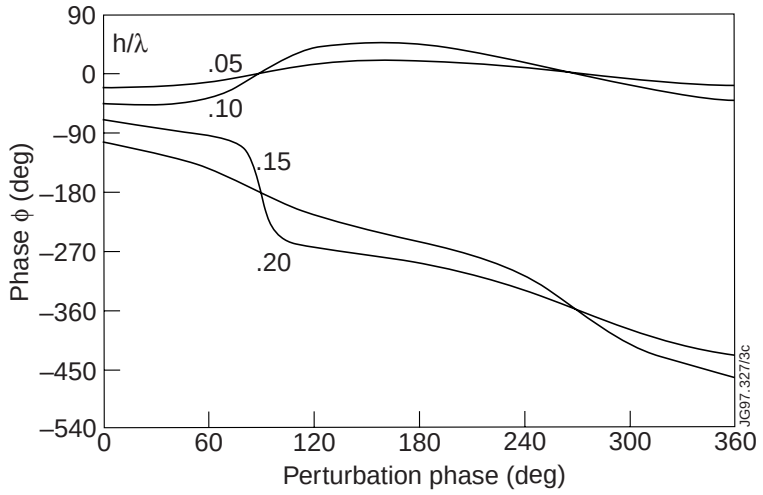

Figure 8: Simulation: Phase run-away occurring with a 2.5^{o} tilt in mean plasma surface when the coherent mode amplitude h/λ exceeds 0.12, $w/\lambda = 2$, $\Lambda/\lambda = 5$.

(e) Certain wavelength bands centred on wavelengths given by $\Lambda/\lambda = m/(2 \sin \theta)$, give enhanced Bragg backscatter. Typically the mean power is a constant -6dB irrespective of the beam width.

(f) For broadband turbulence, mis-alignment introduces a Doppler shifted spectral peak $f_D = 2 f_o v/c \sin \theta$ (the equivalent of phase run-away), figure 9.

(g) Both the phase ϕ_{rms} and power P_{rms}/P_o increase non-linearly with increasing θ, i.e. the signal becomes more incoherent.

(h) $\tilde{\phi}$ and $\tilde{P}$ are correlated (sometimes very strongly) over selected frequency bands (Bragg backscatter).

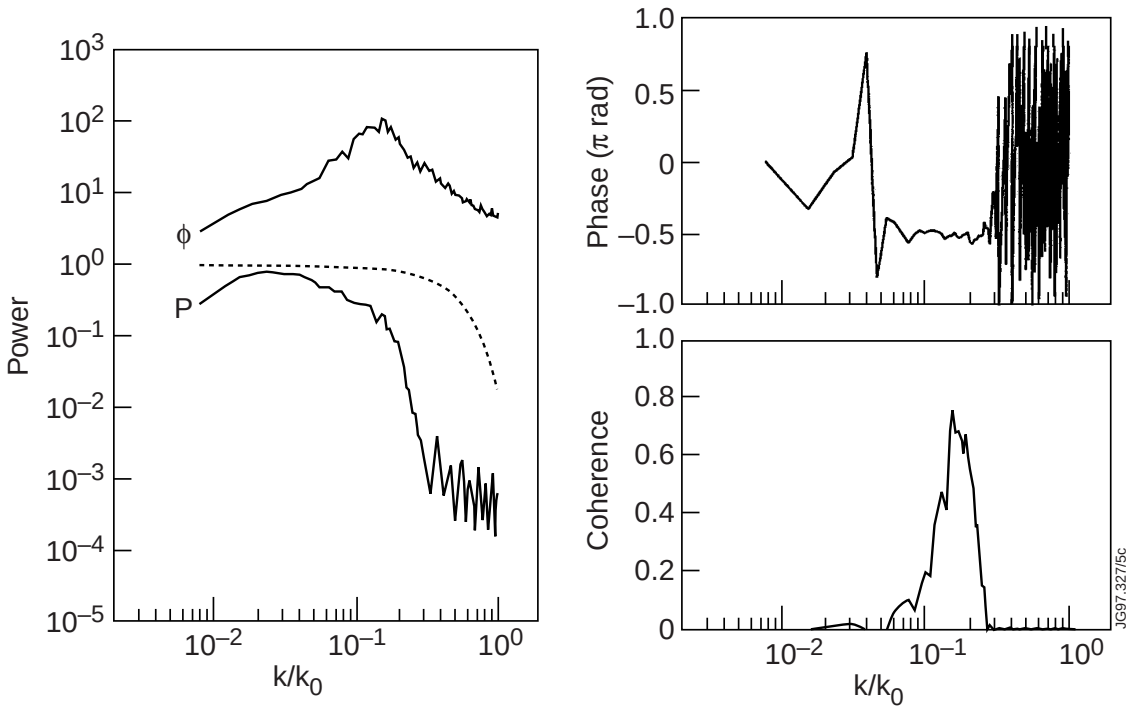

Figure 9: Simulation: Doppler shift in turbulence spectra with incident angle $\theta_1 = 0^o$ and scattered angle $\theta_2 = 8^o$. Note the strong coherence between phase and power fluctuations and relative phase shift of $\pi/2$. The dashed line is the input k-spectrum.

(b) Experimental results.

Data from the JET correlation reflectometer exhibits all of the above features at various times. Figure 10 for example shows the $\gamma^2(f)$ coherence spectrum between $\tilde{\phi}$ and $\tilde{P}$ from a single 75GHz reflectometer channel around the plasma separatrix during an NBI H-mode. It shows a broad coherence from 50 to 200kHz. With a tilt angle of only 2^o the Doppler shift gives a propagation velocity in excess of 4km/s. Asymmetries are more usually evident as differences in fluctuation levels between the adjacent toroidal reflectometer channels, such as the extreme case shown in figure 11 for the 75GHz reflectometer. The phase fluctuations of channel 2 are tiny compared to channel 1, yet the power signal still follows the low frequency oscillation. Note how in channel 1 when the phase rms goes up the mean power goes down. The discrepancies are consistent with an asymmetry of around 2 to 5^o.

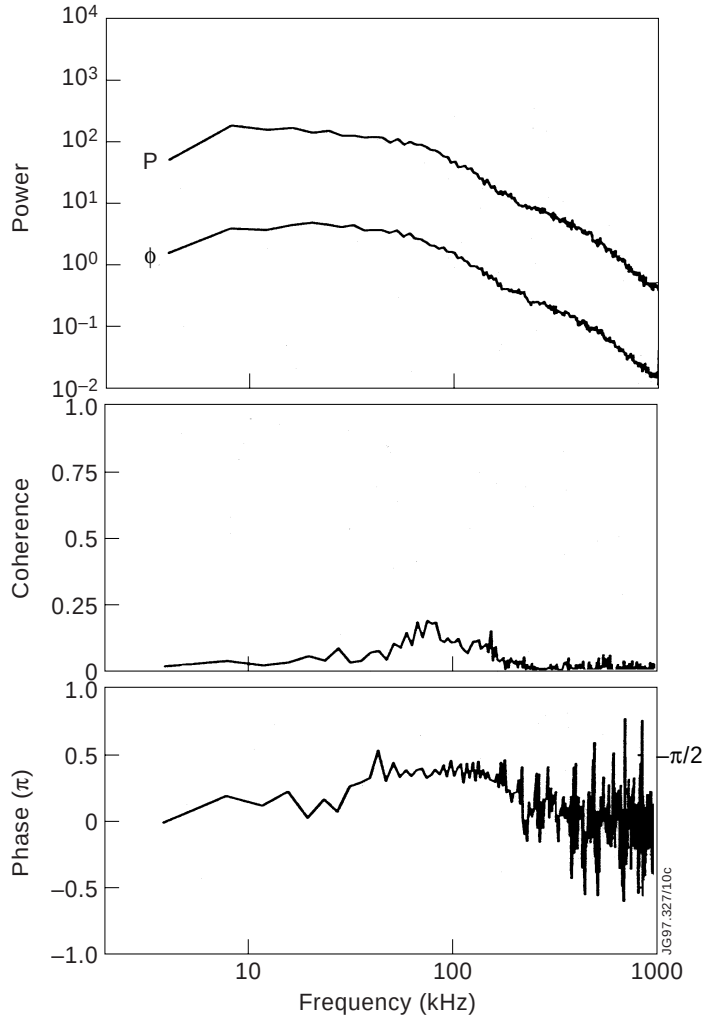

Figure 10: Experiment: $\gamma^2(f)$ coherence and cross-phase spectra between phase and power fluctuations from JET edge. No evident peaks in power spectra but note coherence from 50 to 200kHz and $\pi/2$ phase difference. ϕ_{rms} = 17.3^o, P_{rms}/P_o = 0.51

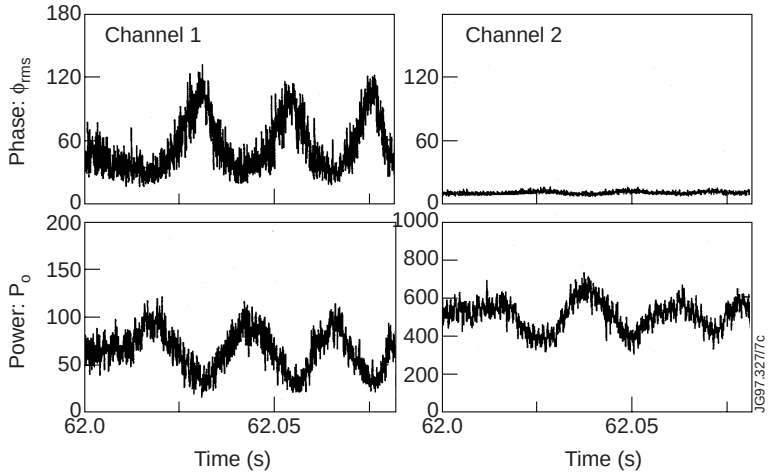

Figure 11: Experiment: Raw signals of rms phase and mean reflected power from two adjacent toroidal reflectometer channels showing evidence of asymmetries in antenna alignment. JET Pulse No. 39325

8. Conclusions

Several models for fluctuation reflectometry have been investigated, but as shown above, the physical optics model provides the first comprehensive explanation of a wide range of fluctuation effects. In fact all fluctuation phenomena observed with the JET correlation reflectometers can be explained and interpreted by the physical optics model. Of course for the JET diagnostic, the short microwave wavelengths, small antennas and large plasma distances make the far-field formulation appropriate. However smaller machines and divertor diagnostics may require near-field solutions - which may reveal new effects.

Acknowledgements

Thanks to J Howard, D V Bartlett, A Costley for stimulating discussions during the development of the model, and on the interpretation of experimental data. The JET data was obtained with the assistance of the members of the JET Task Forces during the 1996 experimental campaign.

References

[1] Irby J H and Stek P, Rev. Sci. Instrum. **61** 3052 (1990)

[2] Conway G D et al, 'Observations on Bragg backscatter from rippled surfaces via reflectometry.' Bull. Am. Phys. Soc. **37** 1453 (1992)

[3] Conway G D, Rev. Sci. Instrum. **64** 2782 (1993)

[4] Conway G D, Schott L and Hirose A, Plasma Phys. Control. Fusion **38** 451 (1996)

[5] Conway G D, Schott L and Hirose A, Rev. Sci. Instrum. **67** 3861 (1996)

[6] Conway G D, Plasma Phys. Control. Fusion **39** 407 (1997)

[7] Conway G D, Vayakis G and Bartlett D V, 'Reflectometer fluctuation and correlation studies on JET.' 3rd Intl. Reflectometer Workshop, Madrid (1997)

[8] Conway G D, 'Effects of asymmetries on reflectometer fluctuation measurements', To be submitted to: Plasma Phys. Control. Fusion (1997)